

# UC Irvine

## UC Irvine Previously Published Works

**Title**

Energetic Ion Experiments in DIII-D

**Permalink**

<https://escholarship.org/uc/item/5gc2g6f1>

**Journal**

Fusion Science & Technology, 48(2)

**ISSN**

0748-1896

**Author**

Heidbrink, WW

**Publication Date**

2005-10-01

**DOI**

10.13182/fst05-a1050

**Copyright Information**

This work is made available under the terms of a Creative Commons Attribution License, available at <https://creativecommons.org/licenses/by/4.0/>

Peer reviewed

# ENERGETIC ION EXPERIMENTS IN DIII-D

W. W. HEIDBRINK\* *University of California, Irvine, California 92697*

Received August 6, 2004

Accepted for Publication September 8, 2004

*A summary of fast ion experiments in the DIII-D tokamak is given. Most of the experiments involve ~80-keV deuterium beam ions. Deceleration of dilute fast-ion populations is accurately described by coulomb scattering theory. Fast waves with frequencies several times the deuterium cyclotron frequency interact with beam ions when the product of wave number and gyroradius  $k_{\perp}\rho_i$  is  $\geq 1.4$ . Global confinement of fast ions is often excellent although sawteeth, tearing modes, and beam-driven instabilities can cause additional transport. Intense beam-ion populations often drive instabilities. Toroidicity-induced Alfvén eigenmodes (TAE) and somewhat lower frequency modes (originally called beta-induced Alfvén eigenmodes) are often observed in a wide variety of plasma conditions. Over 50% of the beam power is lost during strong activity. Damping mechanisms such as mode coupling or radiative damping are needed to explain the observed TAE stability threshold. The most unstable toroidal mode number agrees well with theoretical expectations, but the radial and poloidal structure of the mode and the observed beam-ion transport have not been adequately explained. The modes with frequencies below the TAE are probably two types of energetic particle modes: the resonant TAE and the resonant kinetic ballooning mode.*

**KEYWORDS:** *fast ions, Alfvén eigenmodes, neutral beams*

## I. INTRODUCTION

A typical tokamak plasma contains thermal electrons, thermal ions, and a population of suprathermal fast ions produced by fusion reactions, neutral-beam heating, or radio-frequency heating in the ion cyclotron range of frequencies (ICRF). This suprathermal ion population often provides most of the power that sustains the plasma. Accordingly, an understanding of the basic properties of

the fast-ion population is required to understand the bulk plasma properties. Key issues include how fast energy is transferred to the bulk plasma, what the spatial distribution is of the fast ions, and whether or not the fast ions drive instabilities that degrade their confinement. The results from 30 yr of study of these issues are summarized in review papers by Heidbrink and Sadler<sup>1</sup> and the International Thermonuclear Experimental Reactor (ITER) Energetic Particle Expert Group.<sup>2</sup> One particular instability, the toroidicity-induced Alfvén eigenmode (TAE), was reviewed in Ref. 3. The present review highlights the contributions of the DIII-D group to this body of knowledge following the basic outline of Ref. 1.

The most important energetic ion population in DIII-D (major radius  $R_0 = 166$  cm) is the anisotropic beam-ion distribution associated with injection of ~80-keV deuterium neutrals into the torus. Neutral beam deposition has been studied more intensively elsewhere,<sup>1</sup> but the available spectroscopic measurements are consistent with the conventionally employed cross sections.<sup>4-6</sup> There are two orientations of the beamlines: the so-called “left” beams inject horizontally with a tangency radius of 115 cm and the “right” beams inject horizontally with a tangency radius of 76 cm. The beams usually are injected in the direction of the plasma current (co-injection). For the left beams, nearly all ions are born on passing orbits while, for the right beams, some trapped ions are created. For typical plasma parameters, <10% of the injected power is lost to charge exchange and prompt orbit losses. Also, DIII-D is a low-ripple tokamak (~0.3% at the outer wall) so ripple transport is usually insignificant. On occasion, fusion reaction products and energetic ions accelerated by ICRF have been the object of study. Most studies employ conventional diagnostics such as the volume-integrated neutron rate<sup>7</sup> and neutral particle analyzers.<sup>8</sup>

## II. VELOCITY SPACE

### II.A. Coulomb Scattering

The individual behavior of dilute populations of fast ions (test particles) is well understood.<sup>1,2</sup> Once they are born, fast ions decelerate because of coulomb collisions at the rate predicted by standard small-angle scattering

\*E-mail: wwheidbr@uci.edu

theory. DIII-D measurements of the deceleration and pitch-angle scattering of beam ions are among the most accurate in the literature. Short duration ( $\sim 2$  ms) beam pulses are injected to produce a nearly monoenergetic fast-ion population. The subsequent decay of the neutron rate is readily related to the deceleration rate. The first study using this “beam-blip” technique<sup>9</sup> showed that the energy deceleration rate is consistent with classical theory with the correct parametric dependence on electron temperature and density to within an accuracy of 30%. In a second study,<sup>10</sup> the injection voltage and temperature were varied to study the deceleration rate when drag on thermal ions predominates as well as when electron drag predominates. No systematic dependence on the parameter  $E_b/E_{crit}$  was observed, and the data were consistent with classical theory to within a random error of 25%. ( $E_b$  is the beam injection energy, and  $E_{crit}$  is the energy where drag on thermal ions equals the drag on thermal electrons.) More recently, beam blips were used in conjunction with active charge-exchange measurements to determine the pitch-angle scattering rate.<sup>11</sup> The observed rate was in essentially perfect agreement with classical scattering theory (with estimated random and systematic errors of  $\sim 15\%$ ). The deceleration rate also agreed with classical theory.

In addition to these dedicated experiments, other observations show consistency with coulomb scattering theory. The deceleration rate of 0.8-MeV  $^3\text{He}$  ions and 1.0-MeV tritons was inferred from the “burnup” of these D-D reaction products in secondary d- $^3\text{He}$  and D-T fusion reactions<sup>12</sup>; the observations agree with classical theory to within 20%. A study of edge beam ions showed that the ratio of the deceleration rate to the pitch-angle scattering rate has the expected dependence on electron temperature.<sup>13</sup>

## II.B. ICRF Acceleration

The first ICRF experiments on DIII-D used an antenna that was designed to launch ion Bernstein waves (IBWs). When the launched power exceeded a few hundred kilowatts, a parametric decay instability was observed. When this instability occurred, tails formed in the hydrogen and deuterium distribution functions; the magnitude of the tail correlated with the amplitude of the parametric decay instability.<sup>14</sup>

Subsequently, the IBW antennas were replaced by fast-wave antennas. Fast waves with frequencies of 60 to 120 MHz accelerate injected deuterium beam ions. The wave frequency corresponds to the fourth through eighth cyclotron harmonic of the resonant beam ions. The coupled ICRF power was limited to 1 to 2 MW in most of these experiments.

Multiple diagnostic measurements and parametric studies demonstrate high harmonic ICRF heating of beam ions. Acceleration at the fourth harmonic causes an enhancement of the D-D neutron rate (Fig. 1), perpendicular

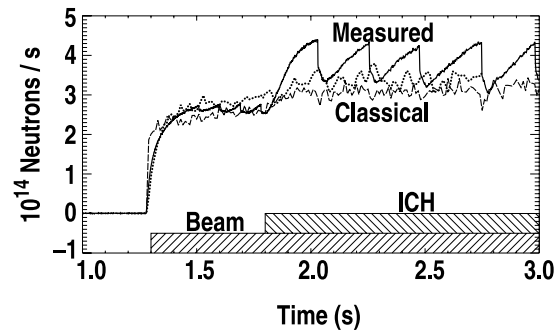


Fig. 1. Time evolution of the neutron emission (solid curve) and two classical predictions that ignore ICRF acceleration (dotted and dashed curves) during high harmonic heating. [Reprinted courtesy of International Atomic Energy Agency, *Nucl. Fusion*, **39**, 1369 (1999).]

ular stored energy, central pressure, and neutral particle flux above 50 keV (Ref. 15). The acceleration is largest when the cyclotron harmonic, including the Doppler shift, is located near the magnetic axis<sup>15,16</sup>. The acceleration increases as the normalized fast-ion gyroradius,  $k_{\perp}\rho_f$ , increases from one to two (Ref. 15). ( $k_{\perp}$  is the perpendicular wave number.) The acceleration is usually smaller at higher harmonic numbers.<sup>15,17,18</sup> For  $k_{\parallel} \neq 0$ , the driven current is reduced when the neutron rate and central pressure are enhanced because the fast-wave power is absorbed by beam ions rather than by current-carrying electrons.<sup>17,18</sup>

Calculations suggest that the beam distribution function is distorted in two ways by the ICRF acceleration: the number of beam ions just below the injection energy increases and a high-energy tail forms.<sup>15</sup> The parametric dependence of the acceleration on gyroradius and harmonic number is explained by the basic properties of the radio frequency diffusion coefficient.<sup>15,19</sup> Fokker-Planck modeling of the observed enhancements in neutron rate and central pressure require an upshift in the parallel wave vector over the vacuum value to obtain quantitative agreement.<sup>19</sup> The calculated fast-wave power absorbed by fast ions is of the correct magnitude to explain the measured decrease in current drive efficiency.<sup>19</sup> Ray tracing calculations using analytical absorption formulas also reproduce the experimentally observed trends.<sup>18</sup>

## III. CONFINEMENT

### III.A. Turbulent Transport

It is well known that turbulent transport of fast ions associated with short-wavelength fluctuations is one to two orders of magnitude smaller than thermal transport,<sup>1</sup> presumably because the large *fast-ion* gyroradius of  $\sim 2$  cm decorrelates the fast ions from fluctuations with a scale

length comparable to the *thermal-ion* gyroradius of  $\sim 0.5$  cm. In the absence of long-wavelength magneto-hydrodynamic (MHD) activity, fusion product and beam-ion confinement in DIII-D is very good, as expected.

In a study of fusion-product confinement,<sup>12</sup> the “burnup” of 0.8-MeV  $^3\text{He}$  ions and 1.0-MeV tritons had the expected parametric dependencies on plasma current, electron temperature, and electron density. The data implied an upper bound for triton diffusion of  $\leq 0.1$  m<sup>2</sup>/s, which is much smaller than the typical thermal value of  $O(1)$  m<sup>2</sup>/s.

As in many other tokamak experiments,<sup>1</sup> the measured neutron rate in DIII-D is often in good agreement with calculations that assume no turbulent transport of the beam ions. The highest fusion yield produced on DIII-D of  $2.2 \times 10^{16}$  n/s is within 10% of the calculated value.<sup>20,21</sup> This level of agreement is observed over two orders of magnitude in the neutron rate for discharges without detectable Alfvén activity or other MHD activity.<sup>22</sup> Similarly, in the absence of significant MHD activity, the current driven by the neutral beams is consistent with calculations that assume neoclassical beam-ion diffusion.<sup>23,24</sup>

### III.B. Effect of Helical Fields and Low-Frequency MHD

As in other tokamaks, a sawtooth crash redistributes the fast ions. The redistribution is inferred from rapid reductions in the fusion reaction rates produced by 0.8-MeV  $^3\text{He}$  ions,<sup>12</sup> 80-keV beam ions,<sup>12,15,25</sup> and  $\sim 5$ -keV deuterons in a Maxwellian distribution.<sup>26</sup> The most recent beam-ion observations<sup>15</sup> are consistent with the standard theory of fast-ion redistribution at a sawtooth crash developed by Kolesnichenko.<sup>27</sup>

Ordinarily, the fishbone instability barely perturbs the D-D fusion reaction rate, indicating that the instability has little effect on beam-ion confinement. The observations<sup>28</sup> suggest that the DIII-D mode is a fluid instability<sup>29</sup> rather than an energetic particle mode.<sup>30</sup> In Ref. 28 it was erroneously reported that fishbones occasionally cause large beam-ion losses, but subsequent measurements<sup>31</sup> showed that TAE instabilities were primarily responsible.

Large tearing modes can degrade beam-ion confinement, causing a reduction in both the neutron rate and the current driven by the neutral beams.<sup>24</sup> Analytical estimates and simulations<sup>32</sup> show that the  $n = 0$  orbit shift (where  $n$  is the toroidal mode number) of the circulating beam ions couples to the helical motion caused by the tearing mode, resulting in islands in the particle’s phase-space that overlap and cause the particle’s motion to become stochastic. In the simulations, the lost neutral beam current drive and neutron emission are 35 and 40%, respectively, in agreement with the measured reductions of  $40 \pm 14\%$  and  $40 \pm 10\%$  (Ref. 32).

An experiment was performed to study the effect of externally imposed helical fields on fusion product con-

finement.<sup>33</sup> The maximum amplitude of the imposed perturbation was limited to  $\sim 9$  G because larger fields caused the plasma to disrupt. These fields, which are an order of magnitude smaller than the tearing-mode field studied in Ref. 32, had no discernable effect on the confinement of 1-MeV tritons. Indeed, helical fields of  $\sim 10$  G are too weak theoretically to induce orbit stochasticity.<sup>33</sup>

### III.C. Electric Fields

For fast ions in tokamaks, the  $E \times B$  drift caused by the radial electric field  $E_r$  is usually of secondary importance compared to the  $\nabla B$  and curvature drifts; however, for ripple-trapped  $\sim 10$ -keV ions in the plasma edge,  $E_r$  can counteract the uncompensated  $\nabla B$  drift and convert ripple-loss orbits into confined orbits.<sup>34</sup> Neutral particle signals associated with this effect were observed on Asdex-Upgrade.<sup>35</sup> A similar experiment on DIII-D failed to reproduce the Asdex results.<sup>13</sup> In DIII-D, edge perpendicular fast-ion orbits are populated when the ratio of the pitch-angle scattering rate to the collisional deceleration rate is sufficiently large.<sup>13</sup>

Radial currents associated with neutral beam injection can charge the plasma, producing radial electric fields. In low density plasmas with negative central shear, the core  $E_r$  inferred from fluctuation measurements forms more rapidly than predicted by neoclassical theory.<sup>36</sup> This rapid formation remains unexplained.

## IV. INSTABILITIES

The beam ion population alters the stability of a large number of modes. The most intensively studied are the TAE (Sec. IV.A), modes with frequencies about half the TAE frequency (Sec. IV.B), and the sawtooth instability (Sec. IV.C). The fishbone instability is sometimes seen, but beam-ion effects seem unimportant.<sup>28</sup> Several beam-driven instabilities are observed but have not yet been studied thoroughly, including Alfvén cascades,<sup>37</sup> ellipticity-induced Alfvén eigenmodes,<sup>15,38</sup> compressional Alfvén eigenmodes or global Alfvén eigenmodes with frequencies just below the cyclotron frequency,<sup>39</sup> and ion cyclotron emission.<sup>31</sup>

### IV.A. Toroidicity Induced Alfvén Eigenmode

The first experimental observations of the TAE occurred concurrently on the TFTR (Ref. 40) and the DIII-D (Ref. 41). Identification<sup>41</sup> was based on Alfvénic scaling of the mode frequency with plasma density, the expected poloidal structure associated with coupling of poloidal harmonics, the central nature of the radial eigenfunction, and evidence that the modes were driven by beam ions. Some features were unexpected, however. Some of the modes had lower frequencies than expected (Sec. IV.B). Instability occurred when the beam speed was slightly

below the Alfvén speed ( $v_f \lesssim v_A$ ), rather than slightly above. In terms of beam beta, the stability threshold was an order of magnitude higher than initially predicted by Fu and Van Dam.<sup>42</sup> All of these surprises were subsequently understood.

The elevated stability threshold prompted a flurry of theoretical activity in search of additional damping mechanisms. Calculations with a global MHD code confirmed that Landau and collisional damping alone could not account for the experimental stability value.<sup>43</sup> Experiments showed that modes with low toroidal mode number  $n$  are stabilized when the mode frequency intersects the Alfvén continuum,<sup>44,45</sup> as predicted by continuum damping theory.<sup>46,47</sup> Local stability estimates suggested that coupling to kinetic Alfvén waves (“radiative” damping<sup>48</sup>) was the dominant damping mechanism and accounted for the observed range of unstable toroidal mode numbers.<sup>38,45,49</sup> An alternative treatment of mode coupling in a global gyrokinetic code also explained the observations; in this theory, coupling to drift kinetic waves in the plasma core is a strong damping mechanism.<sup>50</sup>

Reexamination of the fast-ion drive explained the observed dependencies on  $v_f/v_A$ . Finite orbit width effects broaden the resonance condition so, for typical DIII-D conditions, the wave-particle interaction is strongest when the parallel velocity of the beam ions is  $\sim 0.8v_A$  (Ref. 51), in good agreement with the first experimental observations.<sup>41</sup> Instability had also been observed with even slower fast ions,<sup>45</sup> and theory showed<sup>52</sup> that a sideband resonance at  $v_f = v_A/3$  could also drive the wave.

Reduction of the mode frequency below the nominal TAE frequency is discussed in Sec. IV.B.

The experimentally observed spectrum usually consists of a “cluster” of peaks with steadily increasing toroidal mode number (Fig. 2). The interpretation of this spectral feature is that the various toroidal modes all propagate at the TAE frequency,  $f_{TAE}$ , in the plasma frame but are rotating with the bulk plasma in the laboratory frame, so the observed Doppler-shifted frequency is

$$f_{lab} \approx f_{TAE} + n f_{rot} , \quad (1)$$

where  $f_{rot}$  is the toroidal rotation frequency of the bulk plasma. Reference 53 presents experimental evidence in support of this interpretation. The most compelling evidence comes from a discharge where the toroidal rotation gradually decreased and eventually locked; the frequency separation of the peaks steadily decreased and the cluster collapsed into a single peak when the rotation ceased, in excellent agreement with Eq. (1).

TAEs can cause large losses of beam ions.<sup>41,44</sup> The most detailed experimental investigation of the beam-ion transport employed neutron, plasma pressure, ion-cyclotron emission, and foil bolometer measurements to diagnose the losses.<sup>31</sup> The beam-ion beta tends to saturate near the marginal stability point, so subsequent increases in beam power merely increase the losses. At a

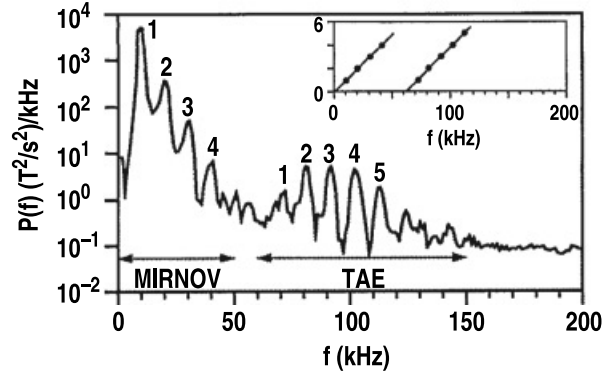


Fig. 2. Typical magnetic spectrum during TAE activity showing a “cluster” of unstable toroidal modes. The splitting of the spectrum is caused by the Doppler shift. The toroidal mode number  $n$  is shown (inset) above the spectral peaks. The inferred TAE frequency in the plasma frame is 63 kHz for this case. [Reprinted courtesy of American Institute of Physics, *Phys. Fluids B*, 5, 2546 (1993).]

given burst, the losses scale linearly with mode amplitude. The losses are concentrated near the outer mid-plane, and the radial step size of a resonant beam ion is roughly 10 cm per toroidal transit. The losses are coherent. Although theory often predicts a diffusive loss process, the observations support a convective “beacon” transport mechanism like the theory<sup>54</sup> developed to explain fishbone losses in the Poloidal Divertor Experiment (PDX).

The TAEs are surprisingly effective in transporting beam ions. A 10% reduction in neutron rate is produced by a mode with 0.1-G amplitude at the Mirnov coil<sup>31</sup>; in contrast, chirping modes (Sec. IV.B) require an amplitude of  $\sim 3$  G to produce a 10% drop, and a 5-G fishbone produces a  $\lesssim 1\%$  drop.<sup>55</sup> The internal amplitude of the TAE measured by soft X-ray diagnostics<sup>41,56</sup> is also very small, implying a peak perturbation amplitude of  $\delta B_r/B_0 \sim 10^{-4}$  (Ref. 56). This perturbation is an order of magnitude smaller than the typical value used in simulations of beam-ion losses by TAEs (e.g., Ref. 57). Indeed, a simulation using the MHD eigenfunction in conjunction with the measured mode amplitude predicted beam-ion losses that are an order of magnitude smaller than the observed losses.<sup>56</sup> More accurate measurements of the TAE eigenfunction and of the beam-ion transport are needed to resolve this discrepancy.

Although TAEs expel beam ions from the plasma under some conditions,<sup>31</sup> more benign redistribution is also observed (e.g., Ref. 58). In fact, under some conditions, the redistribution has a beneficial impact on plasma performance because the redistributed neutral beam current produces a more favorable  $q$  profile.<sup>59,60</sup>

Three studies compared measurements of the TAE eigenfunction with theoretical calculations. A similarity



experiment with NSTX (a similar device with half the major radius of DIII-D) explored the dependence of the most unstable toroidal mode number on geometry and safety factors.<sup>39</sup> The results are in good agreement with the idea that the most unstable toroidal mode occurs when the fast-ion orbital size is comparable to the width of the mode.<sup>51,61</sup> This finding suggests that many modes will be excited in a large burning plasma experiment with the consequence that mode overlap may play a more important role in mode saturation than in current experiments.<sup>62</sup> In a study of the poloidal structure,<sup>63</sup> the data from a poloidal array of magnetic probes were compared with the wavefields predicted by two models: an ideal MHD calculation and a gyrokinetic plasma model that includes coupling to drift-kinetic waves. The phases of the probes disagreed with both theoretical predictions, while the amplitudes agree best with the gyrokinetic model. In a study of the internal structure,<sup>32</sup> soft X-ray measurements were compared with the eigenfunction predicted by ideal MHD, by a gyrofluid model, and by the gyrokinetic model. The measurements indicate a centrally peaked eigenfunction, which is closest to the prediction of the gyrokinetic model.

The eigenfunction, beam-ion loss, and stability studies all point to mode coupling as an important element in the understanding of TAEs in DIII-D. A perturbative approach based on ideal MHD is clearly inadequate. A non-perturbative treatment of the beam-ion pressure and proper inclusion of nonlinear effects may also be important elements in an accurate treatment of Alfvén modes in DIII-D.

Beam-driven TAEs normally occur in bursts. A semi-empirical “predator-prey” model provides an accurate description of the observed experimental trends including the time evolution of the cycle (Fig. 3), the relationship between the peak amplitude and the period of the cycle, and the dependence of the cycle on the neutral-beam fueling rate.<sup>64</sup> The model is based on the idea that

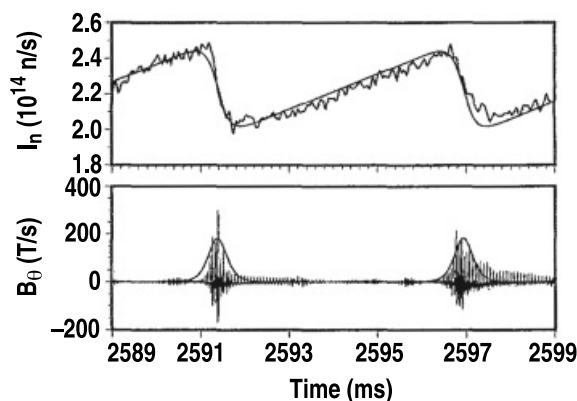


Fig. 3. Neutron rate and mode amplitude during TAE activity. A predator-prey model (smooth curves) fits the cycle. [Reprinted courtesy of American Institute of Physics, *Phys. Fluids B*, 5, 2176 (1993).]

the mode amplitude is the predator that preys on the beam ions; when the beam-ion population declines through losses, the amplitude falls, resulting in a periodic cycle of relaxation oscillations about the marginal stability point. Additional instabilities introduce a perturbation in the evolution equations that disrupts the periodicity of the cycle in a manner that is consistent with experimental observations.<sup>65</sup>

#### IV.B. Energetic Particle Modes

At the time of the first observations of TAEs in DIII-D, modes with lower frequency than expected for the TAE were sometimes observed on magnetic diagnostics.<sup>41</sup> By 1993, it was evident that these lower frequency modes occurred more often in higher beta plasmas.<sup>66</sup> Theoretical analysis of the TAE had indicated that its frequency would decrease into the Alfvén continuum (where it would be heavily damped) as the plasma beta increased,<sup>67,68</sup> but the data of Ref. 66 demonstrated that another instability could appear. MHD calculations showed that a new global eigenmode existed in a gap in the Alfvén continuum associated with plasma compressibility<sup>38</sup>; this mode was dubbed the beta-induced Alfvén eigenmode (BAE) in analogy to the TAE. A toroidal field scan indicated that the frequency of the new mode scaled with the Alfvén speed,<sup>66,69</sup> apparently confirming the identification. The measured mode structure, nonlinear cycle, and beam-ion losses were quite similar for the TAE and the BAE.

Around 1995, three theoretical groups proposed an alternative explanation.<sup>70–72</sup> They suggested that the BAE is a type of energetic particle mode (EPM). An EPM (Ref. 73) differs from a normal mode of the background plasma. An ordinary normal mode (like the TAE) is a weakly damped wave that exists even in the absence of a fast-ion population. In contrast, an EPM is a distinct branch that exists only in the presence of a fast-ion population. Its frequency is determined primarily by the fast-ion distribution function rather than by the background plasma. The eigenfunction resembles the eigenfunction of its related normal mode however.

A 1999 paper provided a comprehensive summary of nearly 10 yr of data.<sup>74</sup> It was found that for this larger dataset, it was impossible to distinguish the frequency of the TAE from the BAE. The observed frequencies varied nearly continuously from  $0.1f_{TAE}$  to the nominal TAE frequency,  $f_{TAE}$ ; moreover, any scaling of the mode frequency with Alfvén speed was weak. Alternative frequency scalings were also inconsistent with the data. The stability properties and fast-ion losses are similar irrespective of the mode frequency.

In 2002, a nonperturbative code compared a particular experimental case with the hypothesis that these lower-frequency modes are two types of EPMS: the resonant TAE and the resonant kinetic ballooning mode.<sup>75</sup> The predicted frequencies, stability properties, and spatial location of the modes were consistent with the

experimental observations. Retrospectively, the strong dependence of mode stability on neutral beam injection parameters and the large variability in mode frequency between successive bursts are qualitatively consistent with identification as EPMS (Ref. 58). Although identification of these modes is not yet definitive, it appears that non-perturbative effects play an important role in Alfvén activity in DIII-D.

Usually, both TAEs and the lower frequency modes have a constant frequency during a burst. On rare occasions, however, the mode frequency “chirps” rapidly downward on a millisecond timescale, in a manner reminiscent of the PDX fishbone.<sup>76</sup> Chirping modes in the TAE range of frequency were first observed on DIII-D (Ref. 55). The spectrum for these chirping modes can span 50 kHz (Ref. 69) or more. The chirping modes can cause large beam-ion losses. They occur in the same frequency band as the BAEs discussed earlier and for similar plasma conditions. Evidently, they also are EPMS but with a different nonlinear saturation mechanism. The origin of this difference is a topic of current study.

#### IV.C. Monster Sawtooth

As in other tokamaks,<sup>1</sup> the fast-ion population produced by ICRF heating can alter the stability of the internal kink mode, producing a monster sawtooth cycle (Fig. 1). Observations in DIII-D (Refs. 15 and 77) are qualitatively consistent with the paradigm articulated by Porcelli<sup>78</sup> and illustrated schematically in Fig. 4. A trapped fast-particle population is produced by ICRF acceleration of the injected beam ions (Sec. II.B). This population provides additional stability against the internal kink. However, as the sawtooth cycle progresses, the growing fast-ion population destabilizes Alfvén instabilities, which tend to clamp the fast-ion pressure. Meanwhile, the plasma current continues to diffuse, lowering the central value of the safety factor  $q_0$  and expanding the  $q = 1$  radius; this increases the MHD drive for the internal kink. Eventually, the fast-particle pressure is insufficient, and a monster sawtooth occurs. Experimentally, the monster sawtooth nearly always occurs for the same value of  $q_0$  and  $q = 1$  radius,<sup>15</sup> confirming the crucial role of current diffusion in the sawtooth cycle. Evolution of the TAE activity probably provides the immediate trigger for the crash, as emphasized in Ref. 77. Future experiments will test the idea that current profile control can prevent the monster sawtooth crash.

#### V. CONCLUSION

To summarize, the most important quantitative contributions of the DIII-D group to the field of energetic ion physics are the following:

1. Dilute populations of fast ions decelerate classically.

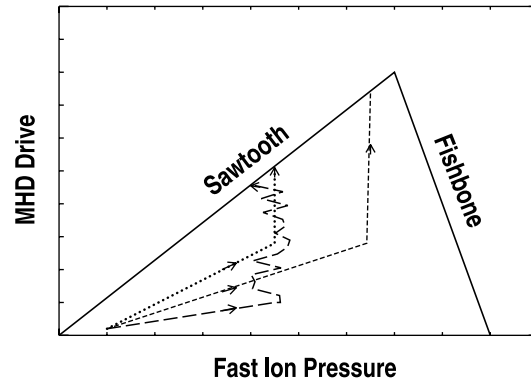


Fig. 4. Diagram illustrating the monster sawtooth cycle. The ordinate represents the ideal MHD energy that drives the sawtooth instability, and the abscissa represents the stabilizing fast ion beta. In the region underneath the triangle, the plasma is stable. If the MHD drive grows too large, a sawtooth crash occurs; if the fast ion beta grows too large, a precessional drift fishbone occurs. The dotted line represents the temporal trajectory during the sawtooth cycle; the MHD drive steadily increases as the current diffuses, but the fast ion pressure stops increasing when a TAE is excited. [Reprinted courtesy of International Atomic Energy Agency, *Nucl. Fusion*, **39**, 1369 (1999).]

2. Heating of large gyroradius ions at frequencies several times larger than the ion cyclotron frequency can be effective.

3. The effect of helical fields on the confinement of circulating fast ions is described by intrinsic orbit stochasticity theory.

4. TAEs are normal modes of the background plasma that can be destabilized by energetic ions. Mode coupling is an important damping mechanism. Fast-ion losses can exceed 50%. Plasma rotation causes a simple Doppler shift of the mode frequency. The relaxation oscillations that occur during strong instability can be explained by a simple predator-prey model. The most unstable toroidal mode number scales as expected.

5. There exists a BAE instability with frequencies lower than the TAE. This instability is probably a type of energetic particle mode.

6. Instabilities with frequencies similar to the BAE can chirp rapidly in frequency.

These results provide a solid scientific basis for projections of fast-ion behavior in ITER and other next step tokamaks. The velocity distribution of alpha particles in burning plasma experiments will be governed by coulomb collisions and, in the absence of strong MHD activity,

the spatial distribution will remain close to the deuterium-tritium fusion reaction profile. Extrapolation of the instability results is more subtle. There are several important differences between neutral beam ions in DIII-D and alphas in ITER (Table I). In particular, the orbit size and beam pressure are often much larger in DIII-D than in ITER, the distribution function is anisotropic, and the beam ions are often sub-Alfvénic. Although these differences make direct simulations of ITER conditions problematic, many key physics issues have been clarified. Linear instability is likely in ITER, especially in higher temperature plasmas with weak magnetic shear.<sup>79</sup> Once instability occurs, the following differences in nonlinear evolution are likely:<sup>62</sup>

1. *Large losses*: Over half of the beam ions are lost under some conditions in DIII-D, but losses should be much smaller with smaller normalized drift orbits and an isotropic population (since a smaller fraction of velocity space will resonate with the waves).

2. *Energetic particle modes*: The large beam pressure and relatively slow fast ions of DIII-D favor destabilization of EPs, but perturbative destabilization of normal modes will probably dominate in a burning plasma.

3. *Nonlinear saturation*: Fast-ion losses often determine the instability amplitude in DIII-D, but in a reactor, the combination of weaker losses and more unstable modes will likely result in more mode coupling.

The DIII-D facility remains a useful testbed for the study of energetic ion physics, particularly the physics of fast-ion driven instabilities. One fruitful approach in future studies is to exploit the flexibility of the device for comparative studies such as the aspect-ratio dependence of different Alfvén instabilities.<sup>39</sup> The ability to control the  $q$  profile (and measure it accurately) is the key ingredient in proposed studies of monster sawteeth and Alfvén cascade modes. Other planned studies hinge on improved diagnosis of the beam-ion distribution function and the spatial structure of the instabilities. Important

TABLE I

Normalized Beam-Ion Parameters in Representative DIII-D Experiments and Projected ITER Values

Parameter	Beam Blip (Ref. 9)	Low $B$ TAE (Ref. 45)	AT EPM <sup>a</sup> (Ref. 58)	ITER (Ref. 80)
Drift orbit $\delta/a$	0.15	0.3	0.15	0.05
Density $n_f(0)/n_e(0)$ (%)	0.3	16	19	0.85
Pressure $\beta_f(0)$ (%)	0.04	8	3.6	1.2
Speed $v_f(0)/v_A(0)$	0.4	1.3	0.4	1.9

<sup>a</sup>Advanced tokamak plasma.

topics that will be addressed with better diagnostics include the following:

1. Why is the TAE so effective in transporting beam ions?
2. Which model of mode coupling (or nonlinear saturation) correctly predicts the observed eigenfunction?
3. Can EPM theory explain the observed dependencies of BAEs on the fast-ion distribution function?
4. What are the key ingredients of a quantitative theory of nonlinear saturation?

For maximum benefit, these experiments should be coordinated with a theoretical program that includes extensive benchmarking of new codes by experimental observations. In particular, codes that predict the full spatial structure of fast-ion driven instabilities with a nonperturbative treatment of the energetic ion population are needed to understand DIII-D results.

In conclusion, DIII-D has contributed significantly to our understanding of energetic ion physics in tokamaks, with particularly strong contributions in the areas of coulomb collisions and beam-driven instabilities. New parameter regimes and improved diagnostics should yield significant new contributions in the future.

## ACKNOWLEDGMENTS

This work was supported by General Atomics subcontract SC-G903402 under DE-FC02-04ER54698. The results in this paper would be impossible without the dedicated effort of the DIII-D team.

This paper summarizes the work done by the DIII-D program in this area over the past 20 yr or more and includes the contributions of many members of the DIII-D Team listed in the Appendix of this volume of *Fusion Science and Technology*.

## REFERENCES

1. W. W. HEIDBRINK and G. J. SADLER, *Nucl. Fusion*, **34**, 535 (1994).
2. ITER PHYSICS EXPERT GROUP ON ENERGETIC PARTICLES, HEATING, AND CURRENT DRIVE et al., *Nucl. Fusion*, **39**, 2471 (1999).
3. K.-L. WONG, *Plasma Phys. Controlled Fusion*, **41**, R1 (1999).
4. R. P. SERAYDARIAN, K. H. BURRELL, and R. J. GROEBNER, *Rev. Sci. Instrum.*, **59**, 1530 (1988).
5. D. F. FINKENTHAL, "The Measurement of Absolute Helium Ion Density Profiles on the DIII-D Tokamak Using Charge Exchange Recombination Spectroscopy," PhD Thesis, University of California at Berkeley (1994).
6. D. G. WHYTE et al., *Nucl. Fusion*, **38**, 387 (1988).
7. W. W. HEIDBRINK, P. L. TAYLOR, and J. A. PHILLIPS, *Rev. Sci. Instrum.*, **68**, 536 (1997).



8. E. M. CAROLIPIO and W. W. HEIDBRINK, *Rev. Sci. Instrum.*, **68**, 304 (1997).
9. W. W. HEIDBRINK, J. KIM, and R. J. GROEBNER, *Nucl. Fusion*, **28**, 1897 (1988).
10. W. W. HEIDBRINK, *Phys. Fluids B*, **2**, 4 (1990).
11. W. W. HEIDBRINK, *Plasma Phys.*, **9**, 28 (2002).
12. H. H. DUONG and W. W. HEIDBRINK, *Nucl. Fusion*, **33**, 211 (1993).
13. W. W. HEIDBRINK et al., *Plasma Phys. Controlled Fusion*, **43**, 373 (2001).
14. R. I. PINSKER, C. C. PETTY, M. PORKOLAB, and W. W. HEIDBRINK, *Nucl. Fusion*, **33**, 777 (1993).
15. W. W. HEIDBRINK et al., *Nucl. Fusion*, **39**, 1369 (1999).
16. R. I. PINSKER et al., "Experiments on Ion Cyclotron Damping at the Deuterium Fourth Harmonic in DIII-D," *Radio Frequency Power in Plasmas: Proc. 13th Int. Conf.*, Annapolis, Maryland, 1999, p. 144, American Institute of Physics (1999).
17. C. C. PETTY et al., "Fast Wave Current Drive in Neutral Beam Heated Plasmas on DIII-D," *Radio Frequency Power in Plasmas: Proc. 12th Int. Conf.*, Savannah, Georgia, 1997, p. 225, American Institute of Physics (1997).
18. C. C. PETTY et al., *Plasma Phys. Controlled Fusion*, **43**, 1747 (2001).
19. M. J. MANTSINEN et al., *Phys. Plasmas*, **9**, 1318 (2002).
20. E. A. LAZARUS et al., *Phys. Rev. Lett.*, **77**, 2714 (1996).
21. E. A. LAZARUS et al., *Nucl. Fusion*, **37**, 7 (1997).
22. W. W. HEIDBRINK, P. L. TAYLOR, and J. A. PHILLIPS, *Rev. Sci. Instrum.*, **68**, 536 (1997).
23. T. C. SIMONEN et al., *Phys. Rev. Lett.*, **61**, 1720 (1988).
24. C. B. FOREST et al., *Phys. Rev. Lett.*, **79**, 427 (1997).
25. E. A. LAZARUS et al., *Phys. Fluids B*, **4**, 3644 (1992).
26. J. A. LOVBERG, W. W. HEIDBRINK, J. D. STRACHAN, and V. S. ZAVERYAEV, *Phys. Fluids B*, **1**, 874 (1989).
27. Y. I. KOLESNICHENKO, V. V. LUTSENKO, R. B. WHITE, and Y. V. YAKOVENKO, *Phys. Plasmas*, **5**, 2963 (1998).
28. W. W. HEIDBRINK and G. SAGER, *Nucl. Fusion*, **30**, 1015 (1990).
29. B. COPPI and F. PORCELLI, *Phys. Rev. Lett.*, **57**, 2272 (1986).
30. L. CHEN, R. B. WHITE, and M. N. ROSENBLUTH, *Phys. Rev. Lett.*, **52**, 1122 (1984).
31. H. H. DUONG et al., *Nucl. Fusion*, **33**, 749 (1993).
32. E. M. CAROLIPIO, W. W. HEIDBRINK, C. B. FOREST, and R. B. WHITE, *Nucl. Fusion*, **42**, 853 (2002).
33. W. W. HEIDBRINK, E. M. CAROLIPIO, R. J. LA HAYE, and J. T. SCOVILLE, *Nucl. Fusion*, **40**, 935 (2000).
34. J. A. HEIKKINEN, W. HERRMANN, and T. KURKI-SUONIO, *Phys. Plasmas*, **4**, 3655 (1997).
35. W. HERRMANN and ASDEX UPGRADE TEAM, *Phys. Rev. Lett.*, **75**, 4401 (1995).
36. T. L. RHODES et al., *Nucl. Fusion*, **39**, 1051 (1999).
37. R. NAZIKIAN, Private Communication (2003).
38. A. D. TURNBULL et al., *Phys. Fluids B*, **5**, 2546 (1993).
39. W. W. HEIDBRINK et al., *Plasma Phys. Controlled Fusion*, **45**, 983 (2003).
40. K. L. WONG et al., *Phys. Rev. Lett.*, **66**, 1874 (1991).
41. W. W. HEIDBRINK, E. J. STRAIT, E. DOYLE, G. SAGER, and R. T. SNIDER, *Nucl. Fusion*, **31**, 1635 (1991).
42. G. Y. FU and J. W. VAN DAM, *Phys. Fluids B*, **1**, 1949 (1989).
43. C. Z. CHENG et al., "Energetic/Alpha Particle Effects on MHD Modes and Transport" in *Plasma Physics and Controlled Nuclear Fusion Research 1994*, Vol. 3, p. 373, International Atomic Energy Agency (1995).
44. E. J. STRAIT et al., "The Stability of TAE Modes in DIII-D" in *Plasma Physics and Controlled Nuclear Fusion Research 1992*, Vol. 2, p. 151, International Atomic Energy Agency (1993).
45. E. J. STRAIT, W. W. HEIDBRINK, A. D. TURNBULL, M. S. CHU, and H. H. DUONG, *Nucl. Fusion*, **33**, 1849 (1993).
46. M. N. ROSENBLUTH, H. L. BERK, J. W. VAN DAM, and D. M. LINDBERG, *Phys. Rev. Lett.*, **68**, 596 (1992).
47. F. ZONCA and L. CHEN, *Phys. Rev. Lett.*, **68**, 592 (1992).
48. R. R. METT and S. M. MAHAJAN, *Phys. Fluids B*, **4**, 2885 (1992).
49. R. R. METT, E. J. STRAIT, and S. M. MAHAJAN, *Phys. Plasmas*, **1**, 3277 (1994).
50. A. JAUN, J. VACLAVIK, and L. VILLARD, *Phys. Plasmas*, **4**, 1110 (1997).
51. G. Y. FU and C. Z. CHENG, *Phys. Fluids B*, **4**, 3722 (1992).
52. R. BETTI and J. P. FREIDBERG, *Phys. Fluids B*, **4**, 1465 (1992).
53. E. J. STRAIT, W. W. HEIDBRINK, and A. D. TURNBULL, *Plasma Phys. Controlled Fusion*, **36**, 1211 (1994).
54. R. B. WHITE et al., *Phys. Fluids*, **26**, 2958 (1983).
55. W. W. HEIDBRINK, *Plasma Phys. Controlled Fusion*, **37**, 937 (1995).
56. E. M. CAROLIPIO et al., *Phys. Plasmas*, **8**, 3391 (2001).
57. Y. TODO, H. L. BERK, and B. N. BREIZMAN, *Phys. Plasmas*, **10**, 2888 (2003).
58. W. W. HEIDBRINK, N. N. GORELENKOV, and M. MURAKAMI, *Nucl. Fusion*, **42**, 972 (2002).
59. K. L. WONG et al., *Phys. Rev. Lett.*, **93**, 085002-1 (2004).
60. K. L. WONG et al., *Nucl. Fusion*, **45**, 30 (2005).
61. B. N. BREIZMAN and S. E. SHARAPOV, *Plasma Phys. Controlled Fusion*, **37**, 1057 (1995).
62. W. W. HEIDBRINK, *Phys. Plasmas*, **9**, 2113 (2002).
63. W. W. HEIDBRINK, A. JAUN, and H. A. HOLTIES, *Nucl. Fusion*, **37**, 1411 (1997).
64. W. W. HEIDBRINK et al., *Phys. Fluids B*, **5**, 2176 (1993).
65. W. W. HEIDBRINK and J. R. DANIELSON, *Phys. Plasmas*, **1**, 4120 (1994).
66. W. W. HEIDBRINK, E. J. STRAIT, M. S. CHU, and A. D. TURNBULL, *Phys. Rev. Lett.*, **71**, 855 (1993).
67. G. Y. FU and C. Z. CHENG, *Phys. Fluids B*, **2**, 985 (1990).
68. D. A. SPONG, J. A. HOLMES, J. LEBOEUF, and P. J. CHRISTENSON, *Fusion Technol.*, **18**, 496 (1990).
69. W. W. HEIDBRINK, E. M. CAROLIPIO, R. A. JAMES, and E. J. STRAIT, *Nucl. Fusion*, **35**, 1481 (1995).
70. S. BRIGUGLIO, C. KAR, F. ROMANELLI, G. VLAD, and F. ZONCA, *Plasma Phys. Controlled Fusion*, **37**, A279 (1995).
71. C. Z. CHENG, N. N. GORELENKOV, and C. T. HSU, *Nucl. Fusion*, **35**, 1639 (1995).

72. R. A. SANTORO and L. CHEN, *Phys. Plasmas*, **3**, 2349 (1996).
73. L. CHEN, *Phys. Plasmas*, **1**, 1519 (1994).
74. W. W. HEIDBRINK et al., *Phys. Plasmas*, **6**, 1147 (1999).
75. N. N. GORELENKOV and W. W. HEIDBRINK, *Nucl. Fusion*, **42**, 150 (2002).
76. K. McGUIRE et al., *Phys. Rev. Lett.*, **50**, 891 (1983).
77. S. BERNABEI et al., *Nucl. Fusion*, **41**, 513 (2001).
78. F. PORCELLI, *Plasma Phys. Controlled Fusion*, **33**, 1601 (1991).
79. N. N. GORELENKOV et al., *Phys. Plasmas*, **10**, 713 (2003).
80. R. V. BUDNY, *Nucl. Fusion*, **42**, 1383 (2002).